

Project ID: **Fly-Radar**

Project Title: *“Low-frequency multi-mode (SAR and penetrating) radar onboard light-weight UAV for Earth and Planetary exploration”*

Call: **H2020-MSCA-RISE-2020**

WP1 – Mars Surface and subsurface analyses and terrestrial analogs

D1.4: Report – Martian Surface and Subsurface Stratigraphic Parameters

Lead contributor	UCBL (P. Allemand, F. Mancini, E. Mariani)
Other contributors	CSFK (A. Kereszturi)

Due date	31/07/2022
Delivery date	22/08/2022
Deliverable type	Report
Dissemination level	PU

Document History

Versio	Date	Description
V1.0	15/07/2022	Draft
V1.1	22/08/2022	Final



1. List of Abbreviations

ASP	Ames Stereo Pipeline
CRISM	Compact Reconnaissance Imaging Spectrometer for Mars
CTX	Context Camera
DTM	Digital terrain model
LDA	Lobate debris apron
MGS	Mars Global Surveyor
MOC	Mars Orbiter Camera
MRO	Mars Reconnaissance Orbiter
MSL Curiosity	Mars Science Laboratory rover Curiosity
THERMIS	Thermal Emission Imaging System

2. Publishable Summary

In this deliverable, we present 5 contexts of Martian geology for which the use of an instrument equivalent to FlyRadar would be necessary to understand the organization and nature of the rock masses in the substratum. We choose these contexts in order they cover most of the geological diversity of the Martian geology. We describe volcanic environments, sedimentary deposits, Aeolian dunes, landslides, impact crater filling, and a case of an impact crater filled with ice covered by Aeolian dunes. For each case, we use the available dataset (images from probes or rovers, Digital Elevation Models already available or computed by us) to describe the geology of the area and propose a synthetic stratigraphic column. These stratigraphic columns will serve as a basis for modeling the response of the FlyRadar instrument that will be carried out and described in the deliverable D1.5.

3. Introduction

The objective of this deliverable is to present some geological contexts of Mars for which the FlyRadar instrument could be necessary to identify the geometric organization of the underground and possibly specify the lithology. The sites were chosen according to their scientific interest and the potential of the FlyRadar instrument sized for penetration down to around 20 m depth with an assumed a vertical resolution of around 0.5 m.

The contexts described in this deliverable have been selected to illustrate the diversity of Martian geology (fig. 1) with a particular focus on the apron debris of the Deuteronilus Mensae region for their potential water ice content and on the craters of impact Vernal, Gusev and Jezero crater for their methane source potential. The other areas are the following. The central part of Valles Marineris is occupied by landslides. Images of their internal geometry and possibly the characteristics of the slid rocks are necessary to specify the conditions and processes during sedimentation. The volcanic activity of Mars is represented by the occurrence of volcanoes of various size and also by lava flows. The precise knowledge of the geometry of these flows is necessary to estimate the viscosity of the lava during their emplacement, and there are lava caves too, mostly invisible directly from above. The wind activity of Mars is marked by the construction of dunes with a geometry similar to that found on Earth. The internal structures of the dunes provide information on wind dynamics and its evolution, and some of them might hold water ice in their interior as paleoclimatic indicator. The former presence of rivers on the surface of Mars is evidenced by the presence of dry beds and, at their termination, characteristic sedimentary structures are visible. The internal geometry of these sedimentary bodies provides information on the dynamics of rivers and therefore makes it possible to define the hydrological conditions that prevailed during their formation.

The geological contexts will first be described based on available data. These data are generally HIRISE imagery data at very high spatial resolution completed with topographic data from which the geometry of the site and possibly the surface texture are defined. Then a stratigraphic column for each contexts is proposed which will serve as a basis for modeling the response of the FlyRadar instrument that will be carried out and described in the deliverable D1.5.



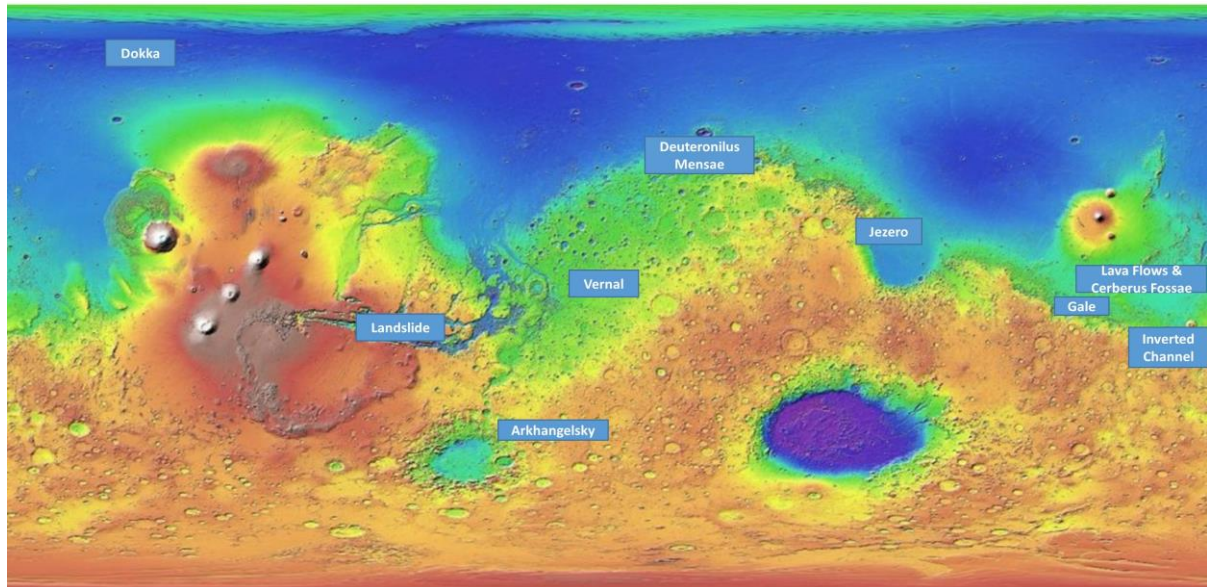


Figure 1: Position of the areas described in this deliverable on a map of the Martian topography (Mola).

4. Results

The 10 sites studied in this document are shown on figure 1. The sites are classified according to the geological context: 1) sedimentary sites, 2) volcanic sites, 3) impact crater sites 4) sites associated with the presence of water ice, 5) Dokka polar crater with infilled icy sediments.

4.1 Sedimentary Contexts

4.1.1 Dunes in Arkhangelsky crater

The Arkhangelsky crater is located northeast of Argyre (fig. 1). This crater has a diameter of about 115 km. It hosts in its northern part a dune field of 312 km² consisting mainly of Barchan dunes indicating a dominant SSW wind. These barchans have kilometric lengths for widths of 300 to 400 m. The heights of these dunes above the bottom of the crater are of the order of 50 m (e.g. Gardin et al. 2011, fig. 2). The bottom of the crater consists of impact breccia without any sedimentary or volcanic deposit.

Hyperspectral data and thermal inertia data associated with the observation of Mars rovers suggest that these sands have a basaltic composition and a grain size between 50 and 500 µm (e.g. Bristow et al., 2018). The interior of the dunes is structured by the avalanches which occur in the downwind face and which are a marker of the advance of the dunes. On terrestrial dunes (e.g. Clayton et al., 2022), the boundaries of the avalanche layers are visible on the radargrams.

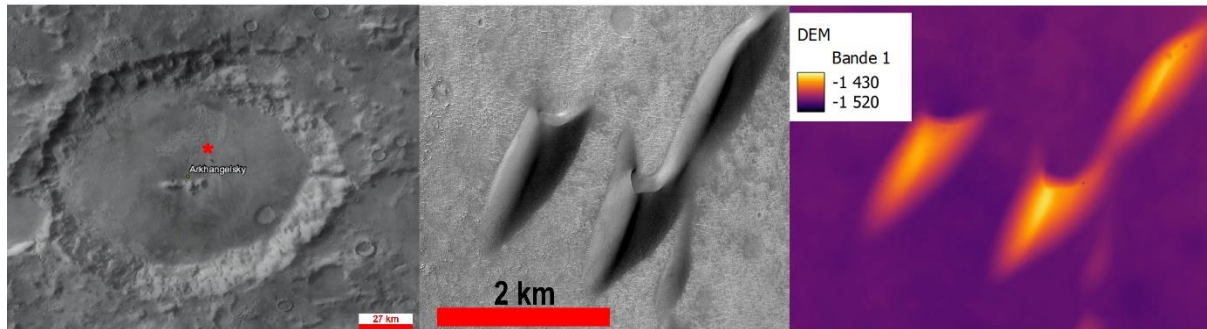


Figure 2 : Arkhangelsky crater on mosaic MGS MOC_WA_Atlas. This impact crater is occupied by a barchane dune field (ESP_054938_1390 Image: NASA/JPL/University of Arizona). Dunes are about 1 km long and 200 m wide and 50 m high above the crater floor (DTEEC_023106_1390_022605_1390_A01 Image: NASA/JPL/University of Arizona).

The bedrock on which the dunes sit consists of a clast-rich breccia whose thickness has been estimated at between 3 and 4 m for the Endeavor crater from data from the Opportunity rover. The Endeavor crater having a diameter of 5 km, this thickness is a minimum for the Arkhangelsky crater whose diameter is 110 km. A possible stratigraphic section is given in figure 3. A layer of sand of regularly decreasing thickness rests on a brecciated substratum resting itself on the rocks present before the impact.

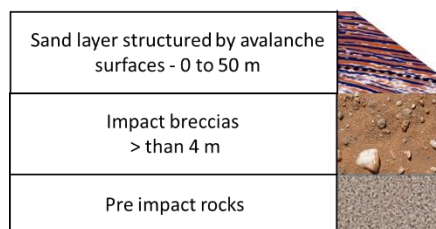


Figure 3: Simplified stratigraphic column of the Arkhangelsky crater.

4.1.2 Giant Landslides in Valles Marineris

The flanks of Valles Marineris Canyon are affected by about 40 landslides of several km³ each (Quantin et al., 2004). These landslides have their source on the flanks of Valles Marineris several kilometers above the bottom of the canyon and each extend over several tens of km² over thicknesses between 5 and 50 m (fig. 4). The internal structure of these landslides is currently inaccessible to observation. The internal structures could be indicative of the role of fluids during the flow (Lajeunesse et al., 2006). The walls of Valles Marineris are mainly made up of igneous and volcanic rocks (Flahaut et al., 2011). The bottom of the canyon is possibly made up of volcanic rocks.

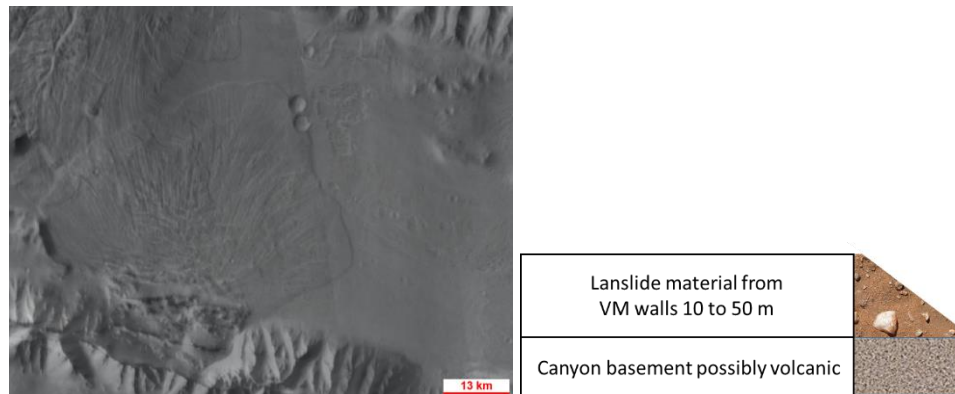


Figure 4: Left: Example of a landslide in Valles Marineris Canyon from the mosaic MGS MOC_WA_Atlas. Right: stratigraphic section.

4.1.3 River deposits

During periods of warmer and wetter climates than present, liquid water flowed on Mars in the form of rivers similar to those found on Earth. These rivers transported and deposited sedimentary material in sedimentary bodies. These sedimentary bodies are good candidates for examination by the FlyRADAR instrument, in order to reconstruct the conditions of their formation. Figure 5 gives an example of such a river whose bed is now in positive relief in the landscape following differential erosion between the bedrock and the indurated bed of the river.

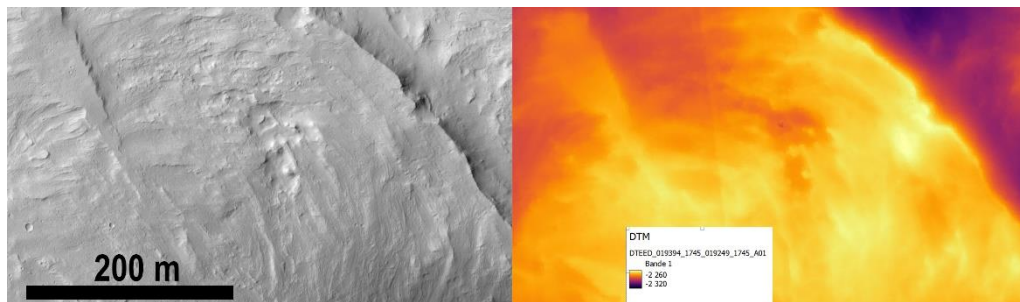


Figure 5: Hirise image and DTM of an paleo meander.

The stratigraphic column is represented in Figure 6, the structured content of the bed, about ten meters thick, rests on a fine substrate, possibly clayey.

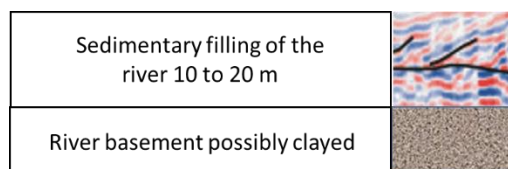


Figure 6: stratigraphic column of a meandering river.

4.2 Volcanic Contexts

4.2.1 Lava flow in Central Elysium Planitia

Central Elysium Planitia is a volcanic plain close to the Elysium volcano. Volcanic activity in the region is moderately young (Vaucher et al., 2009a) and is marked by shield volcanoes that have emitted fluid lava flows that have spread over tens of kilometers (Vaucher et al., 2009b). The composition of the lavas is still debated. The estimation of the viscosity and the threshold of movement of the lava during its emplacement could be used to

propose a range of realistic composition. Figure 7 shows that the lava flows are 200 meters wide. The topography of the flow shows levees that are characteristic of viscoplastic fluids.

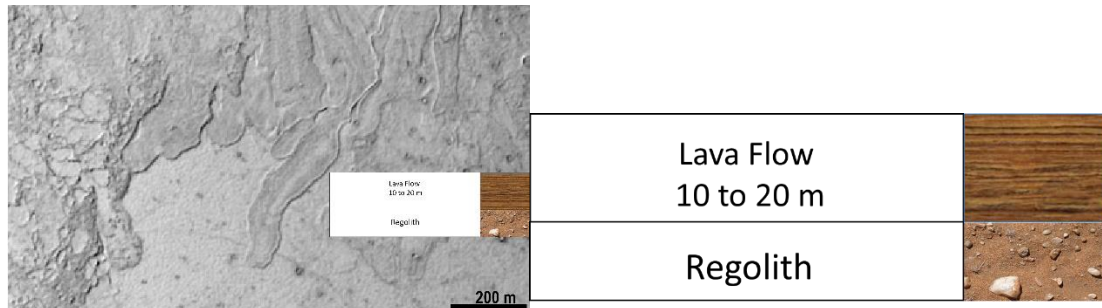


Figure 7: Right: lava flow in Elysium Planitia. Notice the topography of the flows with their characteristic levees. Left: stratigraphic column. CTX image P17_007777_1789_XN_01S199W.

4.2.2 Lava flows in Cerberus Fossae

The Cerberus Fossae region (Fig. 1 and Fig. 88) is characterized by the presence of ESE-WNW oriented open fractures that emitted lavas in the last 200 My. It is also possible that these fractures are the places of emission of water and mud that led to the formation of the Atabasca Valley. Data from the Insight lander's instrument (e.g. Jacob et al., 2022) show that this region is seismogenic. The geometric characteristics of the lavas and possibly muddy deposits are indicative of the rheology of the flows during their deposition, of the speed of emplacement and therefore possibly indicative of their nature. The FlyRADAR instrument will image these areas to determine the thickness and structure of the layers in place and the internal organization of these layers.

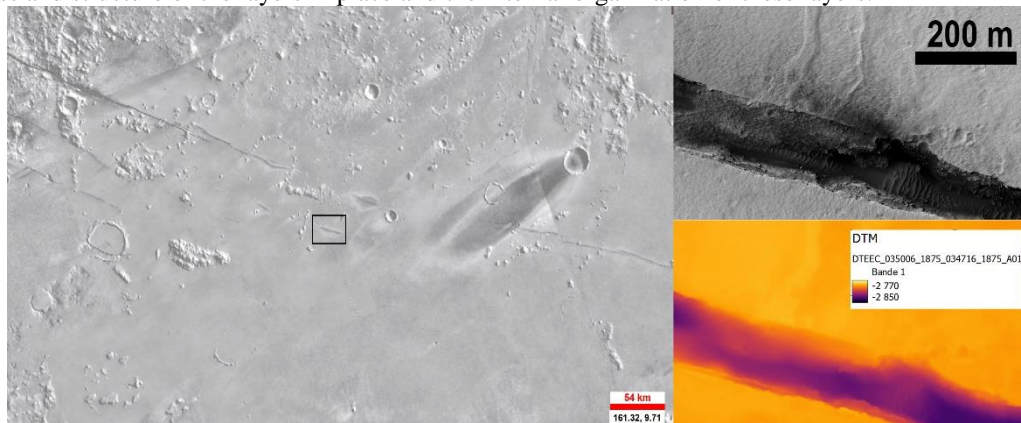


Figure 8: Cerberus Fossae. The area represented left is marked by a rectangle on the general image. Left: MDIM 2.1, upper right: Hirise image ESP_035006_1875, lower right: DTEEC_035006_1875_034716_1875_A01.

A possible stratigraphic section is shown in Figure 8. The layer of lava or mud 10 to 20 m thick rests on a regolith composed of elements whose grain size ranges from one millimeter to one meter.

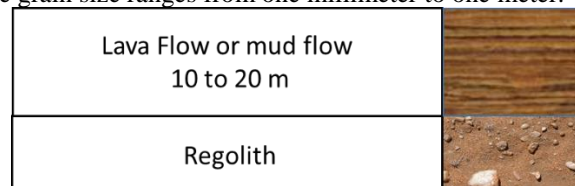


Figure 9: Possible stratigraphic section of Cerberus Fossae

4.3 Impact crater's filling – the example of Gusev, Vernal and Gale

Three impact craters (Gusev, Gale and Vernal crater) were mapped using ArcMap with the following datasets: (1) Context Camera (CTX) mosaics for mapping at a pixel-resolution of ~5.0 m/pixel (2) HiRISE images to investigate small-scale textures and morphologies at ~0.5 m/pixel and (2) Orthophoto and CTX DEM that provides a digital elevation model with a resolution of ~9-11 m/pixel (PSP_009385_1655 and PSP_009886_1655 – Gusev crater ESP_011844_1855 and PSP_002812_1855 – Vernal crater). CTX stereo pair to derive Digital Elevation Model (DEM) has been aligned on the HRSC and MOLA Blended DEM (Ferguson, R.L. et al. 2018) using the NASA Ames Stereo Pipeline (ASP) (Broxton M.J. and Edwards L.J. 2008).

The stratigraphy was made by using the crater size-frequency distribution (CSFD) measurements of these three impact craters are based on CTX mosaic using Craterstat sII and JMARS.

The three impact craters Gusev, Vernal and Gale (fig. 1) were chosen to study in detail the geomorphological indicators of methane on Mars. From the analysis of these craters, characteristic and recurring morphologies such as Stream Channels, bed-lacustrine and bed-aeolian sedimentary deposits have been found, indicating a formation environment evolving over time, capable of accommodating a warm and wet as well as a dry past climate.

Gale (fig. 10) and Gusev (fig. 11) craters are situated at a dichotomy boundary between the North and the South hemisphere of Mars and the origin and age of the Martian crustal dichotomy boundary are fundamental questions that remain unresolved at the present time, besides the fact that are also good indicators for possible methane emission spots.

The analysis made in all of these 3 impact craters concern the use of HiRISE DEMs for Gusev crater (images PSP_009385_1655 and PSP_009886_1655) and Vernal crater (images ESP_011844_1855 and PSP_002812_1855) and MSL Curiosity 2D and 3D photogrammetry models for Gale crater.

A map of each crater has been drawn according to geomorphological criteria indicative of the environment of deposits:

- Sedimentary bed-lacustrine deposits: they are characterized by areas of very low albedo that are darker in colour than surrounding terrains. These sedimentary deposits are characterized by regularly alternating layers.
- Sedimentary bed-aeolian deposits: they are characterized by dunes with low albedo (Gale and Vernal craters).
- Volcanic deposits: characterized by chaotic and knobby terrains. In addition to the particular units that characterize these types of deposits, the various mineralogical analyses carried out using CRISM and THEMIS IR Night and Day image datasets revealed the presence of Opaline silica with digitate textures indicating the possibility of the presence of hot spring deposits or the presence of a hydrothermal environment.

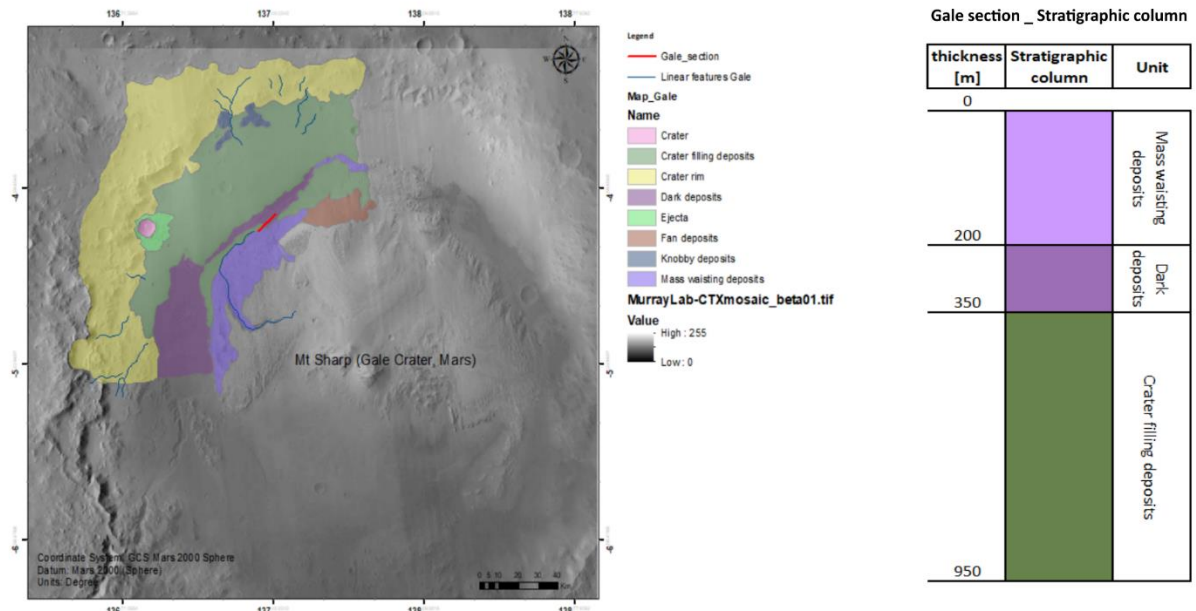


Figure 10: Geological map of the NW border of the Gale crater and possible stratigraphic column. The FlyRadar instrument will be able to image the mass wasting deposit. From these images it will be possible to evaluate the granulometry and lithology of the clasts in the mass wasting deposit.

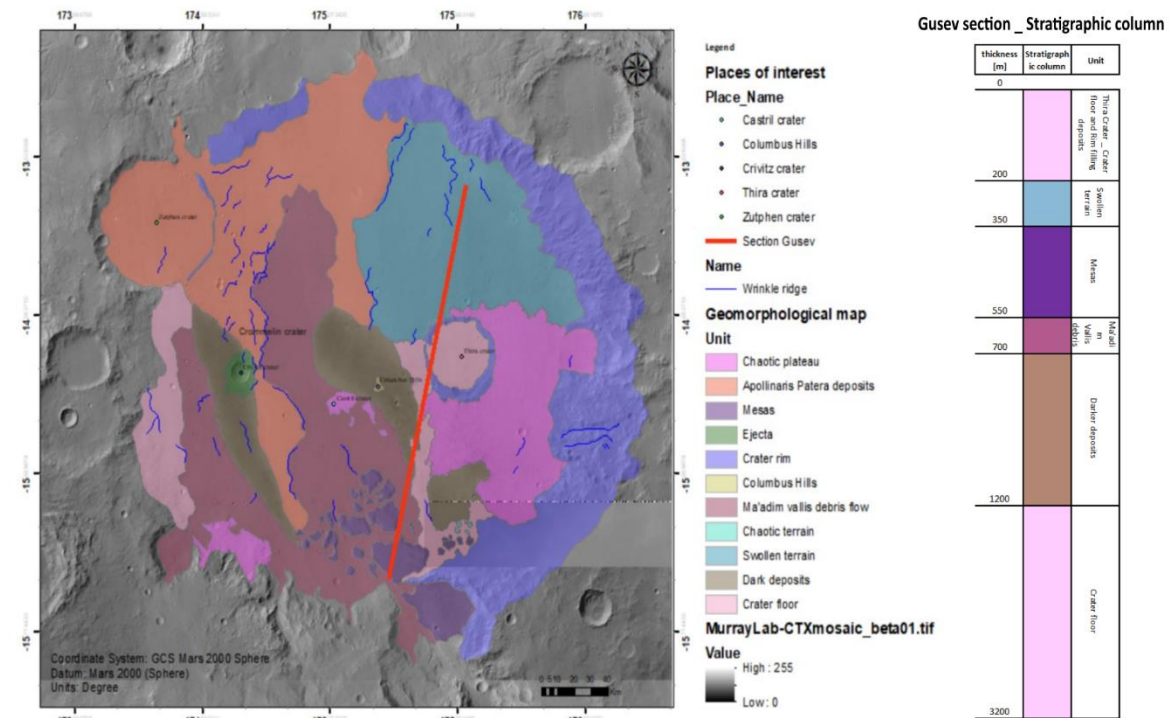


Figure 11: Geological map of the Gale crater and possible stratigraphic column. According to the observation area, the Fly Radar instrument will be able to image the various deposits, and infer their formation conditions.

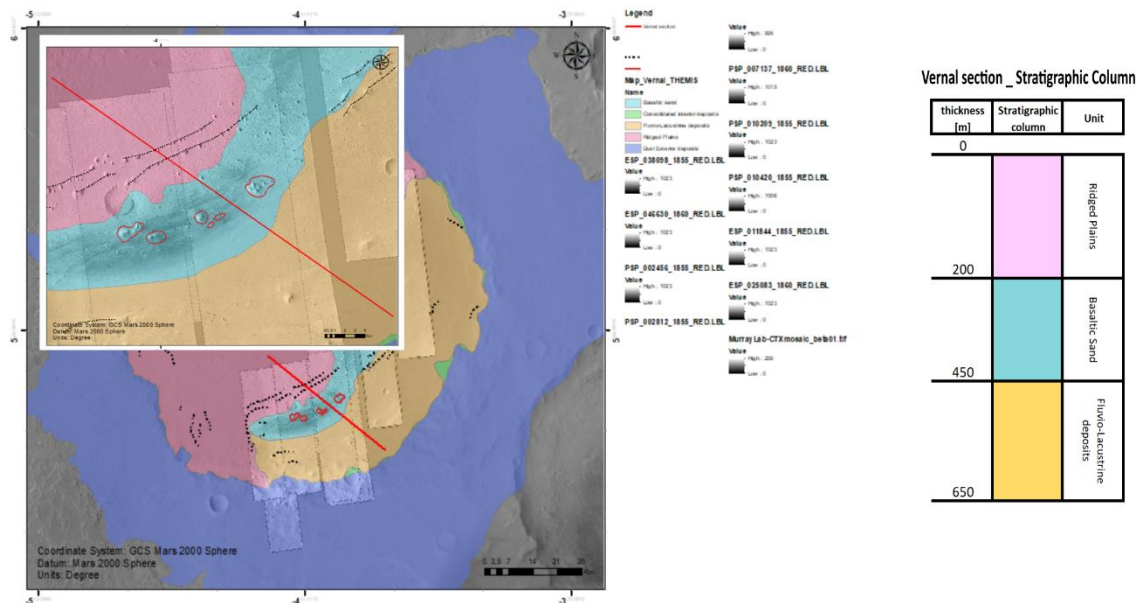


Figure 12: Geological map of the Vernal crater and possible stratigraphic column. According to the observation area, the Fly Radar instrument will be able to image the various units.

4.4 Features related to ice – the lobate debris aprons of Deuteronilus Mensae

To this day, the distribution, morphology, and behavior of glacial and periglacial landforms have been used as key instruments to study small-to-large scale fluctuations in the global climate of Mars (Sharp 1973; Morgan et al. 2009). The transition zone between the north-central parts of Arabia Terra and the Deuteronilus Mensae region (fig. 1) hosts a variety of viscous flow materials that are comparable to morphologies of glacial environments (Van Gasselt et al. 2011). Orbital radar sounding confirms relatively pure ice under a protective lag deposit of lobate debris aprons and lineated valley fill that are commonly observed in this region (Petersen et al. 2018). Deuteronilus Mensae, first defined as an albedo feature at lat 35.0° N., long 5.0° E., by U.S. Geological Survey (USGS) and International Astronomical Union (IAU) nomenclature, is a gradational zone along the dichotomy boundary in the northern mid-latitudes of Mars.

The origin and age of the Martian crustal dichotomy boundary are fundamental questions that remain unresolved at the present time. Several scenarios for its formation, including single and multiple large impact events, have been proposed and debated in the literature. Endogenic processes whereby crust is thinned by internal mantle convection and tectonic processes have also been proposed. Planetary accretion models and isotopic data from Martian meteorites suggest that the crust formed very early in Martian history. Using populations of quasi-circular depressions extracted from the topography of Mars, other studies suggest that the age difference between the highlands and lowlands could be ~100 m.y. Furthermore, understanding the origin and age of the dichotomy boundary has been made more complicated due to significant erosion and deposition that have modified the boundary and its adjacent regions. The resulting diversity of terrains and features is likely a combined result of ancient and recent events

Deuteronilus Mensae was mapped using ArcMap with five individual datasets to provide a high-resolution map of the area: (1) Context Camera (CTX) mosaics obtained by the Murray Lab website as a basis for mapping at a pixel-resolution of ~5.0m/pixel (Dickson et al. 2018); (2) HiRISE images to investigate small-scale textures and morphologies at ~0.5m/pixel and (2) Orthophoto and CTX DEM that provides a digital elevation model with a resolution of ~9-11 m/pixel (B17_016366_2244 and J04_046273_2237). CTX stereo pair to derive Digital Elevation Model (DEM) has been aligned on the HRSC and MOLA Blended DEM (Ferguson, R.L. et al. 2018) using the NASA Ames Stereo Pipeline (ASP) (Broxton M.J. and Edwards L.J. 2008).

It is possible to classify the geomorphological units (fig. 13), into 4 categories. The stratigraphic relation and their internal characteristics could be analyzed and evaluated by a FlyRADAR category instrument.

-*Plateau material*: Cratered highlands with channels, elongated depressions and secondary crater fields. It hosts rimless and infilled craters, sub-circular basins and well-preserved rampart craters. Crater density, elevation, and morphologies indicative of fluvial activity decrease towards north, whereas the abundance of surface collapse features, dissected highland blocks, mesas and remnant knobs located in the lower plains increase. We have distinguished under the term *lower plateau* the dissected plateau material.

-*Plains material*: Relatively smooth plains with variable albedo. Crater densities are lower than on highland materials. The plains display clusters of knobs and hummocky materials. Wind streaks at dark albedo areas are covered by a thin dust mantle, indicating modification by eolian processes

-*Crater material*: We divide ejecta blankets into smaller, well-preserved units that display pronounced lobes and blankets and large, moderately and highly degraded blankets that are partly superposed by younger craters. Crater floors are commonly covered with surficial fill material or glacial-like units like concentric crater fill.

-*Surficial material*: Lobate debris aprons (LDAs) surrounding mesas, knobs and extending from the bases of plateaus into valleys or lowlands. Smooth fill materials display mass wasted deposits of small grain sizes that are embedded between blocks, knobs and channel systems

LDA, as well as the valley and crater fill deposits, are geomorphic indicators of ground ice, and their concentration in Deuteronilus Mensae is of great interest because of their potential association with Martian climate change. The paucity of impact craters on the surfaces of debris aprons and the presence of ice-cemented mantle material implies young (for example, Amazonian) surface ages that are consistent with recent climate change in this region of Mars. SHARAD former recorded radar data across Deuteronilus Mensae suggest that LDAs contain nearly pure ice under a debris cover with a glacial unit thickness between 1 km and 15 m (Morgan, G.A. et al. 2021) maximum reachable limit with radar penetration.

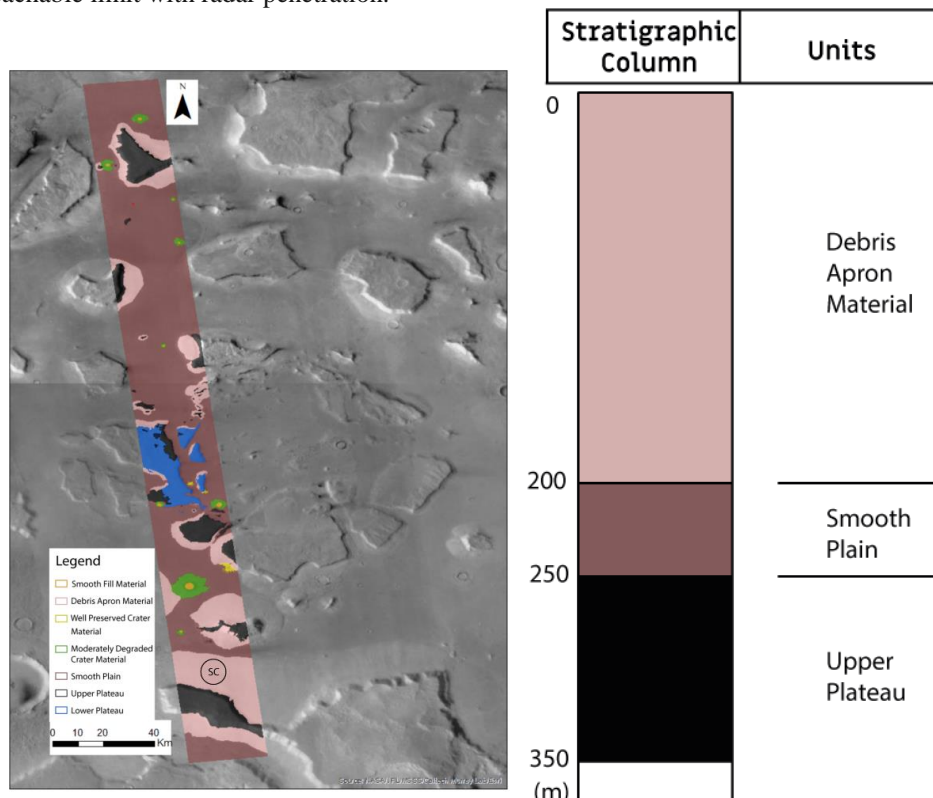


Figure 13: Map of Deuteronilus Mensae showing the main units of the area and stratigraphic units. According to the planned characteristics of the Fly Radar instrument, it will be possible to investigate every unit.

4.5. Ice filled polar crater

Dokka is a 50 km diameter ice (or ice-dust mixture) filled impact crater in the northern circumpolar region of Mars (77.16 N, 214.29E). The bright ice filling in its interior stays there during local summer also. It holds paleoclimatic information on former ice deposition and possible sublimation conditions also. The deepest part of the crater (along its rim) is only at 750 m depth from its rim, however the deepest interior part is filled by the above mentioned ice, around 1 km thickness or more. A huge amount of ice is situated in it, what is probable the remnant of a former larger permanent polar ice cap or polar layered sediments, with many interior layers of different dust content.

The expected sandwich-like stratigraphy at this crater composed of the following units upwards:

- bedrock
- crater interior back fallen regolith
- crater filling ice or ice-dust mixture
- freshest surface frost layer at the southern part overlying the above listed main icy unit

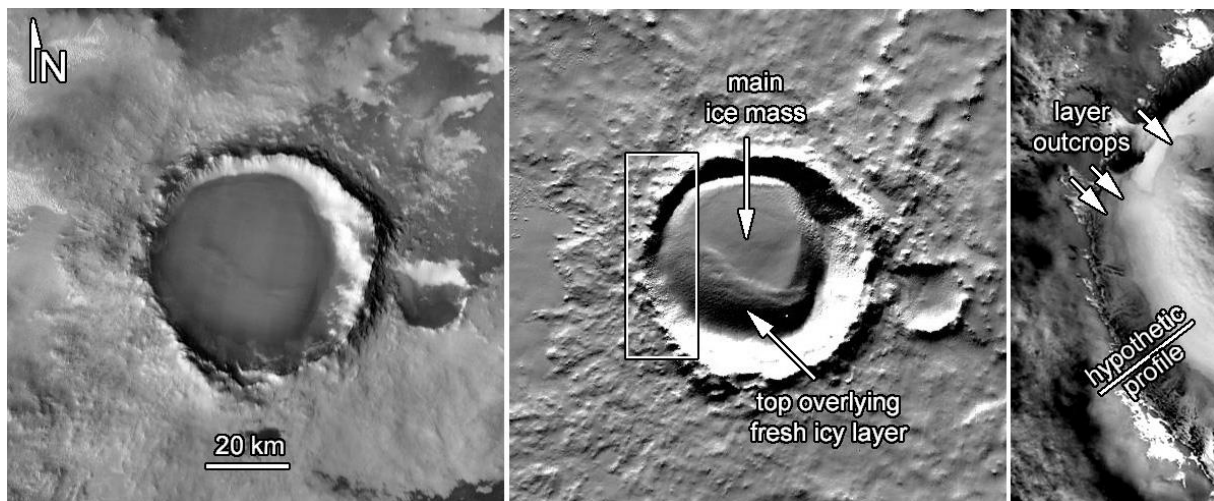


Figure 14: Images of Dokka crater: night-time THEMIS image (left, with cold ice inside), MOLA based shaded relief (middle, with the “pancake” shaped topography of the icy interior deposit), and art of the central sediment on a section of the B02_010240_2575_XN_77N147W CTX image (right) with arrows indicating probable layer outcrops (location of CTX is marked in the middle image).

In case of only shallow radar penetration with surveying only the top 200-300 m thick layers, the edge of the ice filling would be the ideal target for a GPR. A hypothetical section is indicated below. Difference in the back bounced radar signal is expected because the difference in dielectric constant between rocks (below) and ice (above), however the structure of the ice is also not homogeneous, might contain layers and dust embedded, probably also in layered distribution. Different level of cementation, porosity and air bubbles are expected to occur got into the ice structure during airfall based snow deposition. The various layer like interfaces might indicate the cyclicity of frost formation / sublimation and dust lag formation / ephemeral melting or recrystallization driven ice compaction; while the regolith below the ice also expected to be heterogeneous with signatures of pre-ice deposition related early surface processes. The location of the detailed radar analysis could be selected according to the penetration depth, as the thickness of the icy sediment decreases outward.

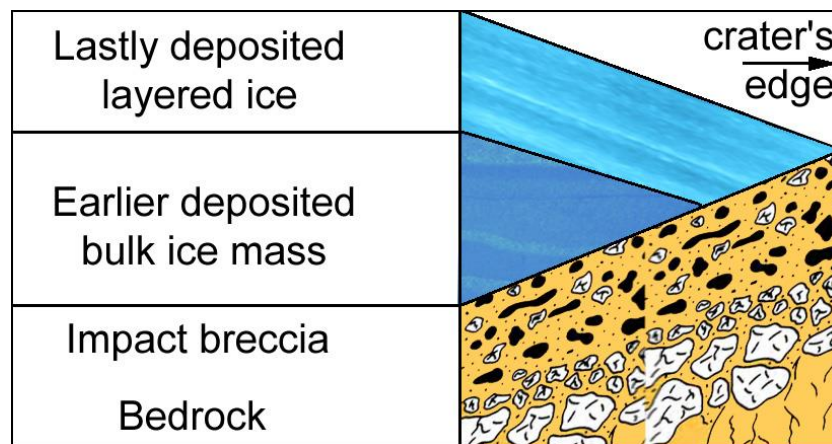


Figure 15. Simplified hypothetical stratigraphic column crossing the edge of the interior ice deposit, along the line indicated in the bottom right of the Figure 14.

5. Conclusion

Nine geological sites on Mars have been described and analyzed in sedimentary and volcanic contexts, linked to impact craters and linked to the presence of ice in the subsurface. For each site, a stratigraphic column was proposed. For sedimentary and volcanic sites, the characteristics of the Flyradar instruments are directly adapted to the study of the internal geometry of the upper layers. For sites related to impact craters and the presence of ice in the underground, the FlyRadar instrument will not be able to image the entire stratigraphic column in a single pass, but still provide important discoveries. It will be necessary to define priorities and/or strategies to best image the basement.

The data collected as part of this work will serve as a basis for modeling the response of the FlyRadar instrument in Martian conditions.

6. References

- Allen, CC., Oehler, D.Z.: A case for ancient springs in Arabia Terra, Mars. *Astrobiology*, 8 (6) (2008), pp. 1093-1112.
- Berard, G., D. Applin, E. Cloutis, J. Stromberg, R. Sharma, P. Mann, S. Grasby, R. Bezys, B. Horgan, K. Londry, M. Rice, B. Last, F. Last, P. Badiou, G. Goldsborough, J. Bell: A hypersaline spring analogue in Manitoba, Canada for potential ancient spring deposits on Mars. *Icarus*, 224 (2013), pp. 399-412, [10.1016/j.icarus.2012.12.024](https://doi.org/10.1016/j.icarus.2012.12.024)
- Bristow, C. S., & Moller, T. H. (2018). Dust production by abrasion of eolian basalt sands: Analogue for Martian dust. *Journal of Geophysical Research: Planets*, 123, 2713–2731. <https://doi.org/10.1029/2018JE005682>.
- Broxton, M.J. and Edwards, L.J.: March. The Ames Stereo Pipeline: Automated 3D surface reconstruction from orbital imagery. In *39th Annual Lunar and Planetary Science Conference* (2008) No. 1391, p. 2419.
- Chuang, F.C. and Crown, D.A.: *Geologic map of MTM 35337, 40337, and 45337 quadrangles, Deuteronilus Mensae region of Mars*. (2009) US Department of the Interior, US Geological Survey.

Clayton K. C., et al.: Near-surface structure of a large linear dune and an associated crossing dune of the northern Namib Sand Sea from Ground Penetrating Radar: Implications for the history of large linear dunes on Earth and Titan. *Aeolian Research* 57 (2022) 100813, <https://doi.org/10.1016/j.aeolia.2022.100813>

Crumpler, L.S., et al. : Results from the first geologic traverse on the topographic rim of a complex impact crater, Endeavour Crater, Mars: *Geology*, (2020) v. 48, p. 252–257, <https://doi.org/10.1130/G46903.1>

Dean, J. F. (2020). Old methane and modern climate change. *Science*, 367(6480), 846–848. <https://doi.org/10.1126/science.aba8518>

Dickson, J.L., Kerber, L.A., Fassett, C.I. and Ehlmann, B.L., 2018, March. A global, blended CTX mosaic of Mars with vectorized seam mapping: A new mosaicking pipeline using principles of non-destructive image editing. In *Lunar and planetary science conference* (Vol. 49, pp. 1-2). The Woodlands, TX, USA: Lunar and Planetary Institute.

Ferguson, R.L., Hare, T.M. and Laura, J.J.U.G.S., 2018. HRSC and MOLA blended digital elevation model at 200m v2, astrogeology PDS annex. US Geological Survey. http://bit.ly/HRSC_MOLA_Blend_v0

Flahaut, J., J.F. Mustard, C. Quantin, H. Clenet, P. Allemand, P. Thomas: Dikes of distinct composition intruded into Noachian-aged crust exposed in the walls of Valles Marineris, *Geophys. Res. Lett.*, 38 (15) (2011), pp. 1-7, 10.1029/2011GL048109.

Gardin, E., et al.: Dune fields on Mars: Recorders of a climate change? *Planetary and Space Science*, *Planetary and Space Science* 60 (2012) 314–321.

Jacob, A, et al.: Seismic sources of InSight marsquakes and seismotectonic context of Elysium Planitia, Mars. *Tectonophysics*, (2022) 837, 229434, 10.1016/j.tecto.2022.229434.

Jaumann, R. et al.: The high-resolution stereo camera (HRSC) experiment on Mars Express: instrument aspects and experiment conduct from interplanetary cruise through the nominal mission, *Planet. Space Sci.*, 55 (7–8) (2007), pp. 928-952.

Kargel, J.S. and Strom, R.G.: Terrestrial glacial eskers: Analogs for martian sinuous ridges. *NASA, Washington, Reports of Planetary Geology and Geophysics Program*, 1990.

Komatsu, G., G.G. Ori, M. Cardinale, J.M. Dohm, V.R. Baker, D.A. Vaz, R. Ishimaru, N. Namiki, T. Matsui: Roles of methane and carbon dioxide in geological processes on Mars. *Planet. Space Sci.*, 59 (2011), pp. 169-181, [10.1016/j.pss.2010.07.002](https://doi.org/10.1016/j.pss.2010.07.002)

Lajeunesse, E., Quantin, C., Allemand, P., & Delacourt, C. (2006). New insights on the runout of large landslides in the Valles-Marineris canyons, Mars. *Geophysical Research Letters*, 33(4), L04403. <https://doi.org/10.1029/2005gl025168>

Luo, Y., M.A. Mischna, J.C. Lin, B. Fasoli, X. Cai, Y.L. Yung : Mars methane sources in northwestern Gale crater inferred from back trajectory modeling. *Earth Space Sci.*, 8 (2021), Article e2021EA001915, [10.1029/2021EA001915](https://doi.org/10.1029/2021EA001915)

Mangold, N., et al.: Chemical alteration of fine-grained sedimentary rocks at Gale crater. *Icarus*, 321 (2019), pp. 619-631, [10.1016/j.icarus.2018.11.004](https://doi.org/10.1016/j.icarus.2018.11.004)

Morgan, G.A., Head III, J.W. and Marchant, D.R.: Lineated valley fill (LVF) and lobate debris aprons (LDA) in the Deuteronilus Mensae northern dichotomy boundary region, Mars: Constraints on the extent, age and episodicity of Amazonian glacial events. *Icarus*, (2009)202(1), pp.22-38, 2009.

Morgan, G.A., Putzig, N.E., Perry, M.R., Sizemore, H.G., Bramson, A.M., Petersen, E.I., Bain, Z.M., Baker, D.M., Mastrogiuseppe, M., Hoover, R.H. and Smith, I.B.: Availability of subsurface water-ice resources in the northern mid-latitudes of Mars. *Nature Astronomy*, (2021), 5(3), pp.230-236.

Oehler, D.Z., Etiope, G.: Methane seepage on Mars: where to look and why. *Astrobiology*., 17 (12) (2017), pp. 1233-1264, [10.1089/ast.2017.1657](https://doi.org/10.1089/ast.2017.1657).

Pajola et al.: Spring deposits and lakeshore layered sediments inside the Vernal crater (SW Arabia Terra): A resource-rich and engineering safe Mars Human Landing site. Ninth International Conference on Mars 2019 (LPI Contrib. No. 2089).

Petersen, E.I., Holt, J.W. and Levy, J.S., 2018. High ice purity of Martian lobate debris aprons at the regional scale: evidence from an orbital radar sounding survey in Deuteronilus and Protonilus Mensae. *Geophysical Research Letters*, 45(21), pp.11-595.

Quantin, C., Allemand, P., Delacourt, C., 2004. Morphology and geometry of Valles Marineris landslides. *Planet. Space Sci.* 52, 1011–1022. <https://doi.org/10.1016/j.pss.2004.07.016>.

Sharp, R.P., 1973. Mars: Fretted and chaotic terrains. *Journal of geophysical research*, 78(20), pp.4073-4083.

Van Gasselt, S., Hauber, E., Rossi, A.P., Dumke, A., Orosei, R. and Neukum, G., 2011. Periglacial geomorphology and landscape evolution of the Tempe Terra region, Mars. *Geological Society, London, Special Publications*, 356(1), pp.43-67.

Vaucher, J., et al.: The morphologies of volcanic landforms at Central Elysium Planitia: Evidence for recent and fluid lavas on Mars. *Icarus* (2009) 200(1) :39-51. 10.1016/j.icarus.2008.11.005.

Vaucher, J., et al.: The volcanic history of central Elysium Planitia: Implications for Martian magmatism. *Icarus* (2009) 204(2):418-442, 10.1016/j.icarus.2009.06.032

Voigt J.R., Hamilton C.W.: Investigating the volcanic versus aqueous origin of the surficial deposits in Eastern Elysium Planitia, Mars. *Icarus*, 309 (2018), pp. 389-410, 10.1016/j.icarus.2018.03.009

Disclaimer: This report reflects only the author's view. The Research Executive Agency (REA) is not responsible for any use that may be made of the information it contains.